

# Tidal Analysis and Implementasion of an Internet of Things (IoT) Sea Level Monitoring Device in Coastal Region

Hollanda Arief Kusuma<sup>1\*</sup>, Farista Egistian<sup>1</sup>, Allsay Kitsash Addifisyukha Cintra<sup>2</sup>,  
Dwi Eny Djoko Setyono<sup>3</sup>

<sup>1</sup>Department of Electrical Engineering, Faculty of Engineering and Maritime Technology,  
Universitas Maritim Raja Ali Haji

Jl. Politeknik Senggarang, Tanjungpinang, Kepulauan Riau, 29115

<sup>2</sup>Research Center for Oceanography, National Research and Innovation Agency

Jl. Pasir Putih Raya No.1, Ancol Timur, Jakarta, Daerah Khusus Ibukota Jakarta, 14430

<sup>3</sup>Research Center for Food Technology and Processing, National Research and Innovation Agency

Jl. Jogja - Wonosari Km. 31,5. Gading IV. Gading. Kec. Playen, Gunung Kidul, Indonesia

Email: hollandakusuma@umrah.ac.id

## Abstract

Monitoring the sea level is crucial for the protection of coastal communities and infrastructure. Instruments that can record and transmit the sea level in real time are essential for preventing potential disasters. This study presents the design, construction, and evaluation of an instrument for measuring sea level using a pressure sensor, a microcontroller, and a GSM module. The sea level analyzed using T Tide analysis. The instrument's accuracy was established through a calibration process, resulting in a sensor reading accuracy of 96.76% and a low root mean square error of 3.24 cm. The linear regression model confirmed the strong correlation between sensor readings and actual water depth, with a coefficient of determination of 0.999. The instrument achieved an accuracy of 96.76% and a low root mean square error of 3.24 cm. Field testing over three days showed the instrument's reliability in measuring sea levels, with an accuracy rate of 91.93% and a root mean square error of 8.07 cm with a packet loss of 7.86%. The study area had mixed semidiurnal characteristics, with water levels ranging from 60.1 cm to 209.55 cm. Significant constituents such as principal lunar diurnal constituent (K1) and Principal lunar semidiurnal (M2) dominate the tidal patterns, each with distinct frequencies, amplitudes, and signal-to-noise ratios. This research provides a precise and cost-effective instrument for measuring water depth, which is suitable for coastal management, environmental monitoring, and scientific investigation.

**Keywords:** accuracy, low-cost, microcontroller, pressure sensor, tidal analysis

## INTRODUCTION

Sea level monitoring is crucial in understanding global climate change's impacts and consequences, such as rising sea levels leading to coastal floods (Takagi *et al.*, 2016). Furthermore, the increase in sea level affects coastal communities and contributes to the increase in natural disasters such as tsunamis and hurricanes (Martínez-Osuna *et al.*, 2021; Van Aalst, 2006). The impacts of sea level rise can be particularly severe for coastal and marine ecosystems. The loss of coastal habitats can lead to habitat contraction, shifts in the geographical location of coastal species, loss of biodiversity, and reduction in ecosystem services (Brierley & Kingsford, 2009; Doney *et al.*, 2012). Moreover, the impact will be greater on small islands (Apdillah *et al.*, 2020; Martyr-Koller *et al.*, 2021). Therefore, accurate and reliable monitoring of sea levels is essential in developing adaptive measures to protect coastal communities and infrastructure (Wang *et al.*, 2020).

Tides are caused by the gravitational pull of the moon and the sun on the Earth's oceans. The rise and fall of tides can vary depending on the location and the alignment of these celestial bodies. Therefore, when monitoring sea levels, it is crucial to account for the influence of tides in order to obtain precise and reliable measurements. Additionally, understanding tidal patterns can also help in predicting extreme events like storm surges and coastal flooding, providing valuable information for coastal communities and disaster management agencies (Williams *et al.*, 2016).

Traditionally, sea level monitoring was performed using tide gauges, which require regular maintenance and calibration to ensure accuracy (Intergovernmental Oceanographic Commission, 2006). However, with the advancement of technology, alternative methods of monitoring sea levels have been developed, including acoustic and pressure sensors. Previous research has demonstrated the feasibility of using acoustic sensors for sea level monitoring (Haq *et al.*, 2021), while other studies have focused on the use of pressure sensors for real-time sea level monitoring (Knight *et al.*, 2021; Kusuma & Oktaviani, 2017; Qiang *et al.*, 2018).

Ultrasonic sensors are commonly used for sea level monitoring. However, ultrasonic sensors have some limitations, such as sensitivity to temperature changes and interference from bubbles and objects in the water (Arshad, 2009). In comparison, pressure sensors are less affected by these factors and provide more accurate readings (Cherqui *et al.*, 2020). Furthermore, pressure sensors can measure sea level changes over a longer period, making them more suitable for monitoring long-term trends in sea level (Talke *et al.*, 2018).

The urgency of using IoT (Internet of Things) platforms for sea level monitoring is apparent, as they provide real-time data, allowing for prompt response to potential disasters or sea level changes (Aziz, 2019; Loftis *et al.*, 2018; Murre *et al.*, 2006). Furthermore, by transmitting data wirelessly, sea level monitoring devices can be easily installed in remote locations, providing valuable information for coastal communities and infrastructure (Apdillah *et al.*, 2021; Knight *et al.*, 2021). For example, IoT platforms such as Thingspeak can store and analyze sensor data from multiple monitoring devices located in different areas (Hsu *et al.*, 2022).

The main objective of this study is to analyze the tidal constituents from the sea level data produced by this device. This study also evaluated a cost-effective, portable sea level monitoring device, leveraging a GSM module for real-time data transmission to the IoT platform Thingspeak. This study assesses the feasibility and accuracy of pressure sensors, which serve as the core components of this monitoring device. By combining these elements, we aim to advance the field of sea level monitoring while providing a valuable foundation for the creation of early warning systems to address the challenges posed by sea level rise in coastal communities.

## MATERIALS AND METHODS

The research was conducted in January 2020 and ended in December 2020. The field test was conducted at Tanjung Siambang, located on Dompok Island in the Riau Islands (as shown in **Error! Reference source not found.**). The field test was conducted over three days, from 8th December 2020 to 10th December 2020. The field test results were used to determine the accuracy and reliability of the device in a real-world setting.

The prototype sea level monitoring device uses the RobotDyn Arduino Mega Pro Mini, a microcontroller with two USARTs for serial debugging and GSM communication. The Maxim DS3231 Real-Time Clock module sends time data via I2C, ensuring accurate and consistent measurement. The G1/4 1.2 MPa water pressure sensor measured pressure values between 0 and 1.2 MPa, with a maximum of 2.4 MPa. Its input voltage was 5 V, and it was connected to the 16-bit ADS1115, converting analog input to digital values. The 16-bit ADS1115 converts water pressure sensor voltage into digital data, ensuring high-resolution conversion for precise measurements. Single-ended 15-bit conversion ensures accurate water pressure and sea level data accuracy.

The ADS1115 uses high-resolution analog-to-digital conversion for precise measurement values, measuring positive voltage with 15-bit resolution. Digital numbers are multiplied by 0.1875 and divided by 1000 to obtain pressure values. The OLED Display 128x64 was chosen due to its lower power consumption and compatibility with I2C. The Micro SD module was utilized for data storage, using the Robotdyn Micro SD shield and a level shifter to convert 5V microcontroller signal to 3.3V microSD voltage. SIMcom's SIM900A GSM module is crucial for sending sea level sensor data

to a server. It operates at 5 VDC and connects to Arduino Mega2560 via serial communication. The Thingspeak platform enables easy prototyping and building of IoT systems without server setup or web software development. Data is sent using a Channel API and GET method, with data sent every 10 minutes.

Component integration begins with the PCB (Printed Circuit Board) design, which is carried out to make the electronic circuit paths neater and reduce the use of jumper wires. After the schematic has been completed, PCB fabrication is then performed. Then, after PCB fabrication, the components are mounted on the PCB (Figure 2). After the components are mounted on the PCB, the next step is to program the Arduino Mega Pro 2560 microcontroller. The programming is done using the Arduino IDE software, where the program code is written in C++.

The program code is responsible for reading data from the sensors, storing data on the Micro SD Card, displaying data on the OLED Display, and sending the data to the server. The flowchart of this instrument can be seen in Figure 3. It's important to note that the system is equipped with error handling capabilities. In the event of a component error, the OLED Display will promptly indicate the issue by displaying a 'Component Error' message. Moreover, the program will cease its execution, ensuring that no further steps are taken, and the instrument will remain inactive to prevent any potential inaccuracies or malfunctions.

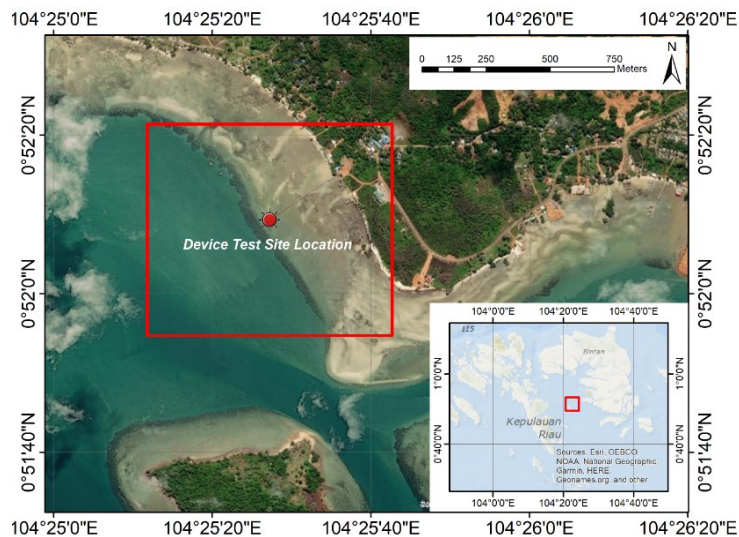


Figure 1. Device Testing Location at Tanjung Siambang

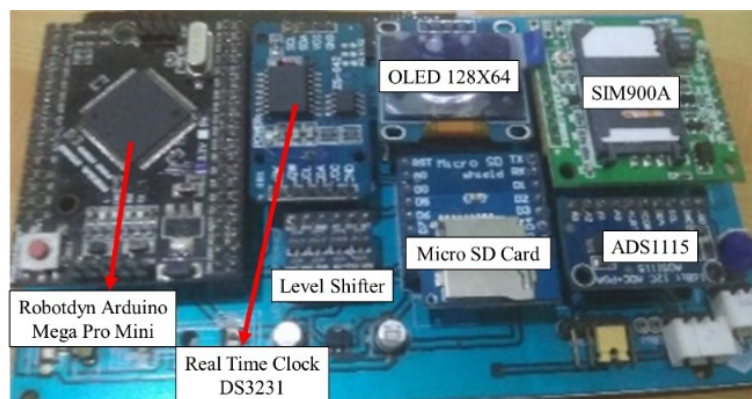


Figure 2. Component Integration Process - Mounting Components on the Printed Circuit Board

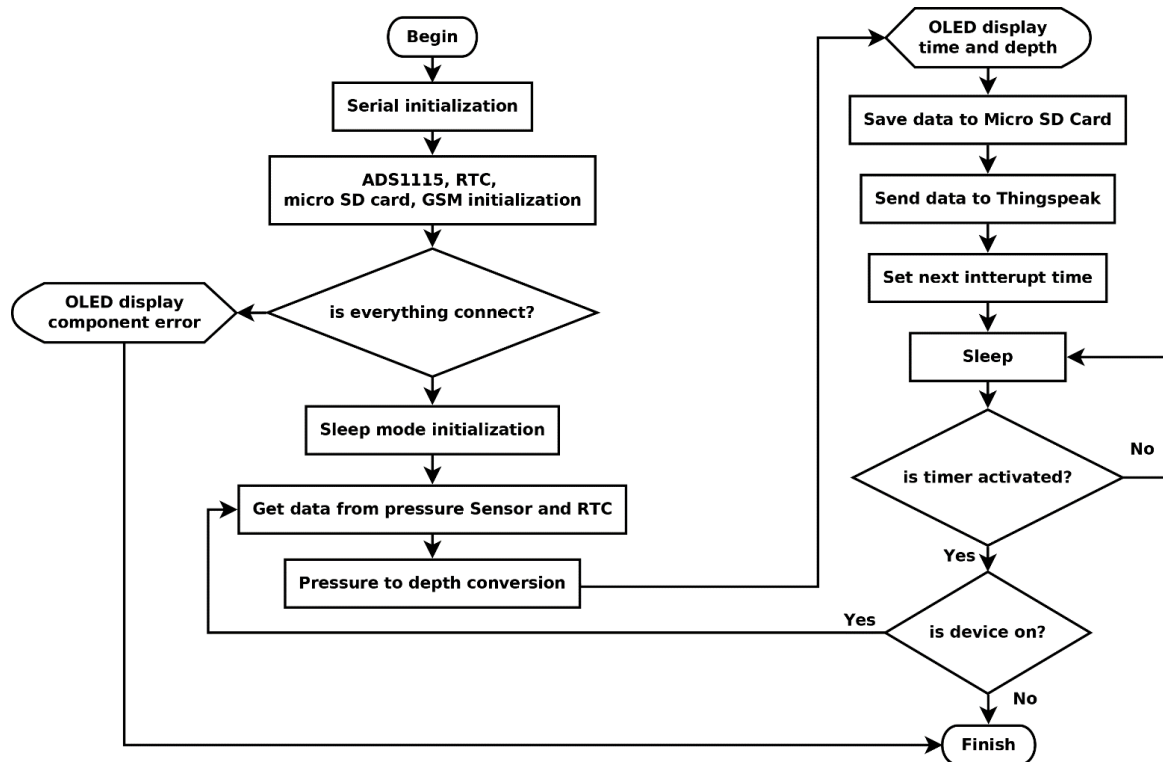


Figure 3. Instrument firmware flowchart

Calibration ensures accurate and reliable readings from sensors, eliminating errors from instrument drift or environmental factors like temperature or pressure changes (Sedha, 2013). A measuring stick is used as a reference to compare sensor results and determine accuracy. This calibration process adjusts the readings obtained from the sensors and eliminates any inaccuracies, thereby improving the overall reliability of the measurement results. The voltage value (V) obtained from the sensor is converted into pressure (p) in MPa units using the Equation 1. The pressure (p) in units of Pa is converted into depth (h) in units of m using the hydrostatic formula (Equation 2) using the density value (ρ) in units of kg.m<sup>-3</sup> and the acceleration of gravity (g) equal to 9.8 m.s<sup>-2</sup>. The measurement error helps ensure that the instrument provides accurate and precise readings of tide levels. The error value is calculated by comparing the data obtained from the calibrator and the sensor using Equation 3. The accuracy of this calibration results is evaluated by comparing it to field data using the Root Mean Square Error (RMSE) method, as calculated using Equation 4. In this evaluation, a lower RMSE value corresponds to superior prediction results (Zhang *et al.*, 2017). Mathematically, the RMSE is determined as follows, with "n" representing the number of data points.

$$p = 125 \times V - 62.5 \tag{1}$$

$$h = \frac{p}{\rho \times g} \tag{2}$$

$$Error = \left| \frac{calibrator\ data - sensor\ data}{calibrator\ data} \right| \times 100\% \tag{3}$$

$$RMSE = \sqrt{\frac{\sum_{i=1}^n (predicted\ value - actual\ value)^2}{n}} \tag{4}$$

A linear curve fitting using inverse method (Lu & Chen, 2007) compares the readings of the water pressure sensor and measuring stick. The regression model, which uses the coefficient of determination (R<sup>2</sup>), is employed to evaluate the fitting (Walpole *et al.*, 2016). The coefficient of

determination ( $R^2$ ) serves as a valuable metric, representing the percent reduction in the total variation observed in the experiment that can be attributed to the use of the regression line.

In simpler terms,  $R^2$  quantifies how effectively the linear regression model explains the variation in the observed data points ( $y_i$ ) concerning their mean ( $\bar{y}_i$ ) and the predicted values ( $\hat{y}_i$ ) from the regression line. A higher  $R^2$  value indicates a stronger correlation and suggests that the regression model provides a better fit to the data, thus accounting for a larger proportion of the variability. This linear regression equation will be integrated into the microcontroller.

$$R^2 = 1 - \frac{SSE}{SST} \tag{5}$$

$$SSE = \sum_{i=1}^n (y_i - \hat{y}_i)^2 \tag{6}$$

$$SST = \sum_{i=1}^n (y_i - \bar{y}_i)^2 \tag{7}$$

The values of sea level measured by the instrument are subject to analysis using descriptive statistics. Descriptive statistics, such as minimum value, maximum value, and average value, provide information about the distribution of the data, which in this case is the sea level measurements. For example, the minimum value gives the lowest water level, the maximum value gives the highest water level, and the average value gives the mean water level.

The sea level data was further analyzed utilizing the T\_TIDE, which is a tidal analysis tool developed by (Pawlowicz *et al.*, 2002). The T\_TIDE uses harmonic analysis to decompose the sea level data into its constituent tidal components. The goal of this analysis was to find the tidal components in the sea water level data, estimate the amplitudes of these identified tidal components, and compare the model output (Xout) from the T\_TIDE with the original site data to find the residual variability. This allows for a more detailed understanding of the variability in sea water levels and helps identify any residual patterns not accounted for by the tidal components.

The significant constituents will be determined by Signal to Noise Ratio (SNR). The SNR is the squared ratio of amplitude to the error in amplitude on every constituent. The SNR cutoff of 2 configured in T\_TIDE to determine the significant constituent. In addition to analyzing sea level values, this research also focuses on packet loss. The percentage of data packets lost can be calculated as the ratio of the number of packets that failed to reach the receiver to the total data sent (Purbakawaca *et al.*, 2022). Packet loss is a critical metric to monitor as it can impact the reliability of the data transmission. The packet loss can be attributed to factors such as low signal strength, which can result in packets being lost if the receiver sensitivity is lower than the signal strength (Archasantisuk *et al.*, 2018).

## RESULTS AND DISCUSSION

The results of this calibration and validation process indicated a high level of accuracy, with the sensor's readings achieving an average percentage error of 7.95%. The Root Mean Square Error (RMSE) was found to be 3.24 cm, demonstrating the reliability of the sensor in accurately measuring water depth. In this linear regression model, the coefficient of determination ( $R^2$ ) was 0.99. An  $R^2$  value of 0.99 indicates that the pressure sensor values and the corresponding water depths have a very strong linear relationship. This high  $R^2$  value means that approximately 99% of the variability in the water depth can be explained by the pressure sensor readings, reinforcing the notion that the sensor is performing well in measuring depth.

The calibration formula utilized in this research was derived from the linear regression equation, which relates the water depth ( $y$ ) in cm obtained from the pressure sensor readings converted to depth in cm ( $x$ ), as shown in Equation 8. The linear regression model was selected to best fit the empirical data. The calibration formula is included in the program to obtain the appropriate depth to obtain the actual water depth.

$$y = 1.02x + 2.33 \quad (8)$$

The field test for the pressure sensor was conducted over a three-day period, encompassing December 8th to December 10th, 2020. A 12V 3.7 Ah Accu battery employed as the primary power source to power the instrument. The sensor was strategically positioned at the outermost point of the pierhead, at an elevation of approximately 3 meters above the seabed. Adjacent to the sensor was a measuring stick. A secure anchoring technique was implemented, which involved the utilization of weights to guarantee the stability and precision of depth measurements. The utilization of the anchoring method proved crucial in effectively preserving the sensor's spatial stability, particularly when subjected to dynamic aquatic environments.

Data taken and transmitted at regular 10-minute intervals throughout the field test. The recorded data were managed and stored in a micro SD card in \*.txt files. These data files included information such as timestamp data, pressure readings in MPa, and corresponding depth measurements in centimeters. The instrument is equipped with a GSM module SIM900A that has been integrated with the Axis operator, enabling real-time data transmission and monitoring. The instrument transmit data to the Thingspeak platform, enabling to access and analyze the collected data in real-time. The measurements of sea level obtained during the field, mean water level, high water level, and low water level were presented on the Thingspeak dashboard (Figure 4).

Throughout the field test, a total of 318 data points were recorded. However, only 293 were successfully transmitted to the server. This discrepancy resulted in a packet loss ratio of 7.86%. The suspected cause of this data loss pertains to issues with the telecommunications provider or the communication server, an aspect that warrants further investigation.

In the study area, a mixed semidiurnal tidal pattern predominates, with two high tides and two low tides occurring in a 24-hour cycle, according to thorough tide observation. Figure 5 provides a visual depiction of the fluctuation in water levels, encompassing the minimum (green), average (yellow), and maximum (red) levels. The figure shows the lowest water level recorded at 60.1 cm, the mean water level recorded at 149.53 cm, and the highest water level recorded at 209.55 cm. This tidal type was similar to the study from Sarmada *et al.*, (2018).

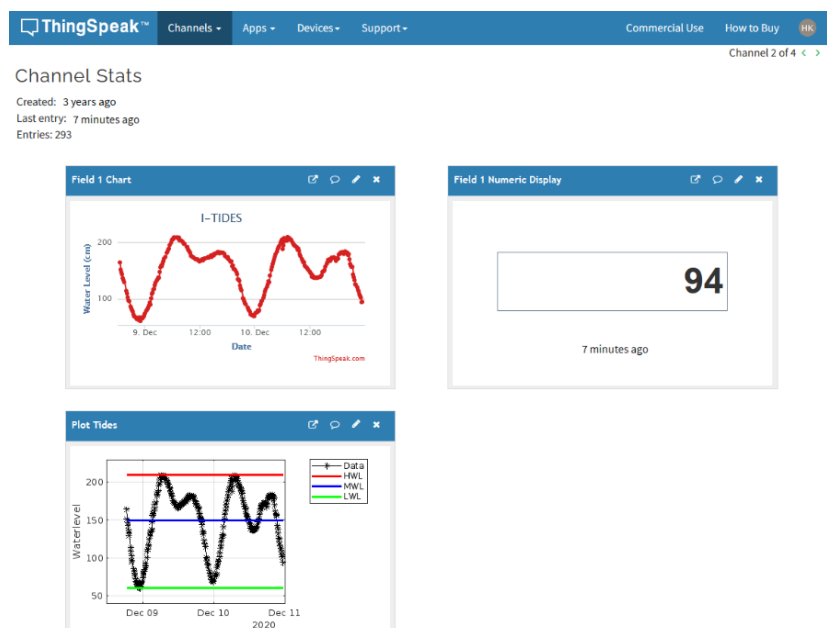


Figure 4. Data Display on Thingspeak Dashboard during Field Test

The amplitudes of the constituent tides are visually represented in Figure 6. This graphical representation further emphasizes the significance of all constituents in sea level variations and highlights their contribution to the overall tidal patterns based on amplitude value. Two constituents were judged to be significant. Two tidal constituents, K1 and M2, emerge as dominant contributors to sea level variations. K1 (Lunar Diurnal constituent), has a frequency of approximately 0.04178 cycles per hour, which corresponds to one full cycle of high and low tides in approximately 24 hours. K1 has a substantial amplitude of 0.4178 m, demonstrates a robust presence, and represents the magnitude of its influence on sea level variations. Similarly, M2 (Principal Lunar Semidiurnal constituent) has a frequency of approximately 0.08051 cycles per hour, which corresponds to two full cycles of high and low tides in approximately 24 hours. M2 has an amplitude of 0.4007m, indicating its substantial impact on tidal patterns. Their high SNR values of 380 and 270, respectively, underscore their reliability and importance. M3 (Principal Lunar Terdiurnal constituent), although not as dominant as K1 and M2, still plays a notable role in sea level variations with a signal-to-noise ratio (SNR) of 3. Although M3 may not have as high an SNR as K1 and M2, its frequency of 0.123 cph and amplitude of 0.0368 m still contribute to tidal patterns, making it a significant component of the tidal cycle.

Based on the tidal analysis, the most significant constituents are the lunar component in the diurnal and semidiurnal bands. The amplitudes of K1 and M2 have a strong influence on the daily tidal patterns observed along coastlines. The significant constituents typically have minimal phase errors (Pawlowicz *et al.*, 2002). Some minor constituents, such as M4, 2MK5, M6, 3MK7, and M8, exhibited lower amplitudes and SNR values. While these constituents may not dominate the tidal signal, their presence contributes to the overall complexity of the tidal behavior.

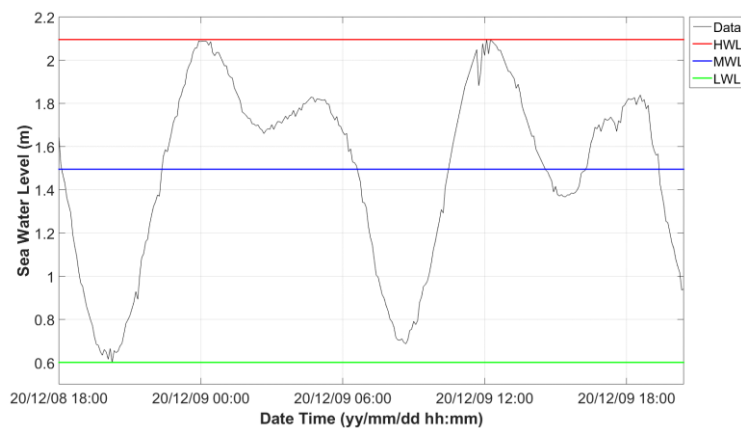


Figure 5. Tides observation result

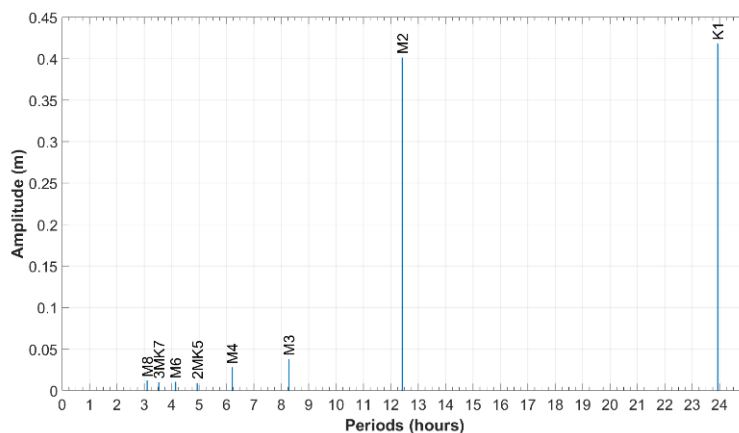
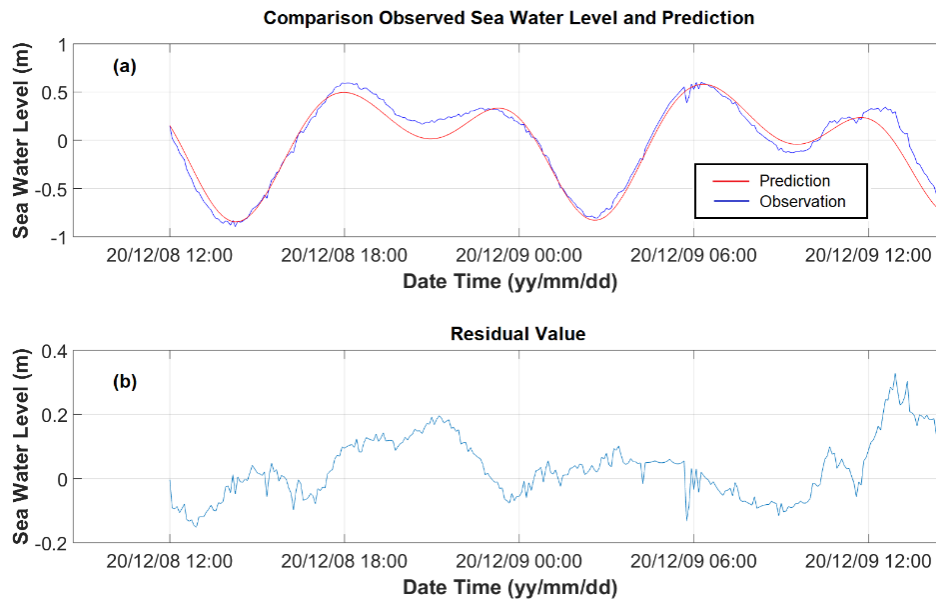


Figure 6. Amplitudes of all tide constituents from the observation





**Figure 7.** Comparison of (a) Observed Sea Water Levels and Tidal Predictions; (b) Residual Values from the comparison

A comparison was performed between the recorded sea water level data and the predictions generated by the T\_TIDE analysis, as shown in Figure 7. The purpose of this comparison was to evaluate the precision of the tidal forecasts in relation to the empirical observations. The tidal predictions generated by the T\_TIDE demonstrated a consistent and periodic pattern. The consistent nature of the predictions demonstrates the effective capture of the fundamental tidal dynamics in our dataset through the analysis.

The fact that this study still has flaw shows how complicated tide dynamics are, which are controlled by many different interactions. Even though the analysis does a good job of capturing the main parts of tides, the fact that there are still some mistakes shows that other factors are at play. Changes in the geography and depth of the water near the coast, as well as changes in the weather, are some of the things that can cause changes in sea level. For example, works by Horrillo-Caraballo *et al.*, (2021), Pirhalla *et al.*, (2022), and Zhu *et al.*, (2019) have shown how weather conditions and local features affect sea levels. In light of these complexities, future study could look into a more thorough modeling approach that takes into account more factors to improve the accuracy of predictions and better understand how sea levels change.

## CONCLUSION

The present study has successfully devised a water depth measurement device by employing a pressure sensor, a microcontroller, and a GSM module. The device demonstrated a notable level of precision, with a reading accuracy of 96.76% and a minimal root mean square error (RMSE). The dependability of recording sea levels in the research area was established through field testing, which resulted in a packet loss rate of 7.86%. The equipment detected tidal characteristics that exhibited a combination of semidiurnal patterns, with fluctuations spanning from 60.1 cm to 209.55 cm. The affordability of pressure sensors renders them suitable for a wide range of applications, particularly in settings with limited resources. The examination of the instrument's tidal patterns identified two primary constituents, namely K1 and M2, which significantly contribute to the fluctuations in sea level. Nevertheless, the presence of residual errors in projections implies that there may be regional fluctuations and meteorological variables that are not adequately considered and may contribute to these discrepancies. The instrument's capacity for extensive



utilization and continued enhancement may result in expanded applications within the fields of oceanography and environmental science.

## REFERENCES

- Apdillah, D., Jaya, I., Iqbal, M., Deswati, R., Glagah, M., Kusumah, B., Nugroho, A. T., & Syafi'i, I. (2021). The Bintan MOS development: contribution of ideas to realize Nusantara marine observation network. *Depik*, 10(1), 53–59. doi: 10.13170/depik.10.1.18181
- Apdillah, D., Pratomo, A., Azizah, D., Nugraha, A. H., & Febrianto, T. (2020). Potency, status and carrying capacity of coral reef ecosystem for sustainable marine ecotourism development; A case study of small islands in Kepulauan Riau-Indonesia. *IOP Conference Series: Earth and Environmental Science*, 584(1), 012007. doi: 10.1088/1755-1315/584/1/012007
- Archasantisuk, S., Aoyagi, T., Kim, M., & Takada, J. (2018). Temporal correlation model-based transmission power control in wireless body area network. *IET Wireless Sensor Systems*, 8(5), 191–199. doi: 10.1049/iet-wss.2016.0109
- Arshad, M. R. (2009). Recent advancement in sensor technology for underwater applications. *Indian Journal of Marine Sciences*, 38(3), 267–273. [https://nopr.niscpr.res.in/bitstream/123456789/6203/1/IJMS 38%283%29 267-273.pdf](https://nopr.niscpr.res.in/bitstream/123456789/6203/1/IJMS%2038%283%29%20267-273.pdf)
- Aziz, A. (2019). Coastal alerting IoT system in response to high tides and turbulent weather. *2019 10th International Conference on Computing, Communication and Networking Technologies, ICCCNT 2019*, pp.1–7. doi: 10.1109/ICCCNT45670.2019.8944838
- Brierley, A. S., & Kingsford, M. J. (2009). Impacts of Climate Change on Marine Organisms and Ecosystems. *Current Biology*, 19(14), R602–R614. doi: 10.1016/j.cub.2009.05.046
- Cherqui, F., James, R., Poelsma, P., Burns, M. J., Szota, C., Fletcher, T., & Bertrand-Krajewski, J. L. (2020). A platform and protocol to standardise the test and selection low-cost sensors for water level monitoring. *H2Open Journal*, 3(1), 437–456. doi: 10.2166/h2oj.2020.050
- Doney, S.C., Ruckelshaus, M., Emmett Duffy, J., Barry, J.P., Chan, F., English, C.A., Galindo, H.M., Grebmeier, J.M., Hollowed, A.B., Knowlton, N., Polovina, J., Rabalais, N.N., Sydeman, W.J., & Talley, L. D. (2012). Climate Change Impacts on Marine Ecosystems. *Annual Review of Marine Science*, 4(1), 11–37. doi: 10.1146/annurev-marine-041911-111611
- Haq, N.A., Khomsin, & Pratomo, D.G. (2021). The Design of an Arduino Based Low-Cost Ultrasonic Tide Gauge with the Internet of Things (IoT) System. *IOP Conference Series: Earth and Environmental Science*, 698(1), 012004. doi: 10.1088/1755-1315/698/1/012004
- Horrillo-Caraballo, J.M., Yin, Y., Fairley, I., Karunaratna, H., Masters, I., & Reeve, D.E. (2021). A comprehensive study of the tides around the Welsh coastal waters. *Estuarine, Coastal and Shelf Science*, 254, 107326. doi: 10.1016/j.ecss.2021.107326
- Hsu, Y.L., Tsai, H.L., & Lu, G.H. (2022). Development of Wireless Multi-Sensor Module for Monitoring Environment of Smart Manufacturing Workplace. *2022 61st Annual Conference of the Society of Instrument and Control Engineers*, pp.797–802. doi: 10.23919/SICE56594.2022.9905821
- Intergovernmental Oceanographic Commission. (2006). Manual on Sea Level Measurement and Interpretation, Volume IV: An Update to 2006. *IOC Manuals and Guides No.14, Vol. IV; JCOMM Technical Report No. 31*. <https://www.oceanbestpractices.net/handle/11329/213>
- Knight, P., Bird, C., Sinclair, A., Higham, J., & Plater, A. (2021). Testing an “IoT” Tide Gauge Network for Coastal Monitoring. *IoT*, 2(1), 17–32. doi: 10.3390/iot2010002
- Kusuma, H. A., & Oktaviani, N. (2017). Electronic design and simulation of low cost ocean tides monitoring instrument using Labcenter Proteus. *Journal of Applied Geospatial Information*, 1(2), 63–68. doi: 10.30871/jagi.v1i2.431
- Loftis, J.D., Forrest, D., Katragadda, S., Spencer, K., Organski, T., Nguyen, C., & Rhee, S. (2018). StormSense: A new integrated network of IoT water level sensors in the smart cities of Hampton roads, VA. *Marine Technology Society Journal*, 52(2), 56–67. doi: 10.4031/MTSJ.52.2.7
- Lu, T., & Chen, C. (2007). Uncertainty evaluation of humidity sensors calibrated by saturated salt solutions. *40*, 591–599. doi: 10.1016/j.measurement.2006.09.012
- Martínez-Osuna, J.F., Ocampo-Torres, F.J., Gutiérrez-Loza, L., Valenzuela, E., Castro, A., Alcaraz, R., Rodríguez, C., & Ulloa, L.R. (2021). Coastal buoy data acquisition and telemetry system for

- monitoring oceanographic and meteorological variables in the Gulf of Mexico. *Measurement: Journal of the International Measurement Confederation*, 183, 109841. doi: 10.1016/j.measurement.2021.109841
- Martyr-Koller, R., Thomas, A., Schleussner, C.F., Nauels, A., & Lissner, T. (2021). Loss and damage implications of sea-level rise on Small Island Developing States. *Current Opinion in Environmental Sustainability*, 50, 245–259. doi: 10.1016/j.cosust.2021.05.001
- Mourre, B., Crosnier, L., & Le Provost, C. (2006). Real-time sea-level gauge observations and operational oceanography. *Philosophical Transactions of the Royal Society A: Mathematical, Physical and Engineering Sciences*, 364(1841), 867–884. doi: 10.1098/rsta.2006.1743
- Pawlowicz, R., Beardsley, B., & Lentz, S. (2002). Classical tidal harmonic analysis including error estimates in MATLAB using TDE. *Computers and Geosciences*, 28(8), 929–937. doi: 10.1016/S0098-3004(02)00013-4
- Pirhalla, D.E., Lee, C.C., Sheridan, S.C., & Ransibrahmanakul, V. (2022). Atlantic Coastal Sea Level Variability and Synoptic-Scale Meteorological Forcing. *Journal of Applied Meteorology and Climatology*, 61(3), 205–222. doi: 10.1175/JAMC-D-21-0046.1
- Purbakawaca, R., Yuwono, A. S., Subrata, I.D.M., Supandi, & Alatas, H. (2022). Ambient Air Monitoring System with Adaptive Performance Stability. *IEEE Access*, 10(2), 1–1. doi: 10.1109/access.2022.3222329
- Qiang, L., Bing-Dong, Y., & Bi-Guang, H. (2018). Calculation and Measurement of Tide Height for the Navigation of Ship at High Tide Using Artificial Neural Network. *Polish Maritime Research*, 25(s3), 99–110. doi: 10.2478/pomr-2018-0118
- Sarmada, I.F., Jaya, Y.V., Putra, R.D., & Suhana, M.P. (2018). *Dinamika Maritim Pemodelan Pola Arus di Kawasan Pesisir Pantai Kawal Kabupaten Bintan*. 7(1), 1–10.
- Sedha, R.S. (2013). *Electronic Measurements and Instrumentation*. S CHAND & Company Limited.
- Takagi, H., Esteban, M., Mikami, T., & Fujii, D. (2016). Projection of coastal floods in 2050 Jakarta. *Urban Climate*, 17, 135–145. doi: 10.1016/j.uclim.2016.05.003
- Talke, S.A., Kemp, A.C., & Woodruff, J. (2018). Relative Sea Level, Tides, and Extreme Water Levels in Boston Harbor From 1825 to 2018. *Journal of Geophysical Research: Oceans*, 123, 1–20. doi: 10.1029/2017JC013645
- Van Aalst, M.K. (2006). The impacts of climate change on the risk of natural disasters. *Disasters*, 30(1), 5–18. doi: 10.1111/j.1467-9523.2006.00303.x
- Walpole, R.E., Myers, R.H., Myers, S.L., & Ye, K. (2016). *Probability & Statistics for Engineers & Scientists: MyStatLab Update* (C. Hoag (ed.); ke-9).
- Wang, Y., Yu, Y., Zhang, Y., Zhang, H.R., & Chai, F. (2020). Distribution and variability of sea surface temperature fronts in the south China sea. *Estuarine, Coastal and Shelf Science*, 240, 106793. doi: 10.1016/j.ecss.2020.106793
- Williams, J., Horsburgh, K.J., Williams, J.A., & Proctor, R.N.F. (2016). Tide and skew surge independence: New insights for flood risk. *Geophysical Research Letters*, 43(12), 6410–6417. doi: 10.1002/2016GL069522
- Zhang, Q., Wang, H., Dong, J., Zhong, G., & Sun, X. (2017). Prediction of Sea Surface Temperature Using Long Short-Term Memory. *IEEE Geoscience and Remote Sensing Letters*, 14(10), 1745–1749. doi: 10.1109/LGRS.2017.2733548
- Zhu, X., Meng, L., Zhang, Y., Weng, Q., & Morris, J. (2019). Tidal and Meteorological Influences on the Growth of Invasive *Spartina alterniflora*: Evidence from UAV Remote Sensing. *Remote Sensing*, 11(10), 1208. doi: 10.3390/rs11101208